Thermal and exergy analysis of optimal performance and refrigerant for an air conditioner split unit under different Iraq climatic conditions

Ali Lateef Tarish[a],*, Mushtaq Talib Hamzah[b], Wasan Assad Jwad[c]

[a] Thermal Mechanics Eng. Dept., Eng.Technical College-Basra, Southern Technical University, Basra, Iraq
[b] Electromechanical Systems Eng. Dep., Thiqar Technical College, Southern Technical University, Iraq
[c] Thermal Mechanics Eng. Dept., Eng.Technical College-Basra, Southern Technical University, Basra, Iraq

ARTICLE INFO

ABSTRACT

In this study, thermal and exergy performance analyses for an air conditioner split unit (ACSU) operating with R-161 were analysed under different Iraq climatic conditions to change the recently worked refrigerants R-134a and R-22. Thermal and exergy analyses were performed under indoor and outdoor environmental temperatures that varied from 30 °C to 55 °C and 17 °C to 27 °C, respectively. An analysis through thermal and exergy was performed to guide the thermodynamic improvement for the ACSU. A comprehensive parametric study was also conducted to investigate the effects of indoor and outdoor temperatures on performance and exergy destruction in each component of the ACSU. The exergy destruction and flow of the compressors, condenser, evaporator and expansion device were calculated to obtain the exergy efficiencies of the ACSU. The Engineering Equation Solver software program was used to develop the ACSU and obtain the thermodynamic refrigerant properties. The improvement of the total exergy efficiencies of the ACSU working with R-161 was found to be 8.6% more than that of the ACSU working with R-22 or R-134a. Results indicated that the average enhancement of coefficient of performance with R161 was 7.3% more than that when R-134a or R-22 was used under the same operating conditions.

1. Introduction

Thermal energy analysis is a good method when investigating any thermodynamic process. This method can improve the process and is the source for developing the exergy analysis. Moreover, this method discovers the energy utilised and consumed in the thermodynamic process. The exergy analysis, which provides an accurate observation of the thermodynamic process, is also based on the first and second laws of thermodynamics. Thermodynamic processes in an actual vapour compression refrigeration system (AVCRS) occur when the heat is rejected and absorbed in the condenser and evaporator with the surroundings.

The irreversibility in an AVCRS is due to the temperature difference between a system and the indoor or outdoor environment. The increases of irreversibility in the AVCRS cause a low coefficient of performance (COP). A thermal and exergy analysis must be applied to determine the maximum COP. This step must be conducted due to the evolution heat transfer loss and exergy destruction for all thermodynamic processes.

The AVCRS is mainly incorporated in air conditioning units, such as an air conditioner split unit (ACSU). Most important specified factors in thermal systems are the amount of energy consumed, refrigerant type, size and cost. In this study, the problem of selecting the ACSU's effectiveness with a suitable refrigerant can be solved by applying thermal analysis and exergy evaluation because the COP varies with the change in the refrigerants.

The strict enforcement of the Kyoto and Montreal protocols [1] has prevented manufacturers from producing HFC refrigerants, such as R-22 and R134a, due to their high global warming potential (GWPs) and ozone depletion potential (ODP). Novel replacement refrigerants should have good properties, such as inflammable, environmentally friendly and high COP. The refrigerant industry is trying to replace HFCs by finding new refrigerants that have low ODP and GWPs and environmentally friendly. The alternative refrigerant fluoroethane (R-161) has ODP = 0 and GWP = 4 (Table 1). Yang et al. [2] discussed the limitations of the flammable R-161. The results show that the low flammability of R-161 can be satisfied by decreasing the working temperature, which varied from 55 °C to −5 °C. The principles of exergy analysis can be found in references [3-7]. Many researchers, such as [8,9], have reported studies using an exergy analytical method for an AVCRS. The research undertaken for alterative refrigerants is

---

Nomenclature

Symbols

CR	Compression ratio (-)
h	Enthalpy (kJ/kg)
$\dot{m}$	Flow rate of mass (kg/sec)
s	Entropy (kJ/kg.K)
T	Temperature (°C)
T_o	Dead state temperature (°C)
T_{sup}	Superheat temperature (°C)
T_{sub}	Subcooling temperature (°C)
$T_{outdoor}$	Outdoor temperature (°C)
T_{indoor}	Indoor temperature (°C)
P	Pressure (kPa)
P_o	Dead state pressure 101.352 kPa
Q_{evap}	Capacity (kW)
Q_{cond}	Heat reject in condenser (kW)
x	Dryness friction (-)
W	Work of compressor (kJ/kg)
$\dot{W}$	Power of compressor (kW)

Subscripts

$evap$	evaporator
$cond$	condenser
$comp$	compressor

d	destruction
exp	expansion
gen	generation
l	Liquid
v	Vapor
exp	Experimental

Greek Symbols

ψ	Exergy (kW)
ψ_{dest}	Exergy destruction
ψ_{Total}	Total exergy destruction (kW)
ψ_{comp}	Exergy destruction in compressor (kW)
ψ_{cond}	Exergy destruction in condenser (kW)
ψ_{evap}	Exergy destruction in evaporator (kW)
ψ_{ex}	Exergy destruction in expansion (kW)
η_{exergy}	Exergy efficiency (%)

Abbreviations

$ACSU$	Air Conditioner Split Unit
$AVCS$	actual vapor compression refrigeration system
COP	Coefficient of performance
GWP	Global warming potential
ODP	Ozone depletion potential
TR	Ton refrigeration

summarised in Table 2. Previous investigations (i.e. from 2005 to 2020 [10-20]) have utilised alternative refrigerants to R22 and R134a in air conditioning systems, such as R290, R502, R407C, R404A, R422A, R410A, R417A, R417B, R123, R417A, R422A, R422D, R424A, HFO-1234yf and HFO-1234ze.

Literature about the use of R-161 in ACSUs is scarce. Several studies have reported the use of the refrigerant mixtures with R-161 (Table 2). However, an analysis of the thermal and exergy with only R-161 is yet to be reported. The literature review has provided thermal and exergy analyses of AVCRS working with different refrigerants. However, the investigation has focused on room air conditioning without considering the indoor and outdoor temperatures. Meanwhile, minimal consideration has been given to the examination of the energy performance and exergy efficiency of ACSUs working in many different climatic conditions. In this research, the thermal and exergy analysis for an ACSU using R-161, as an alternative to R-22 and R-134a, is achieved for different indoor and outdoor environmental temperatures. The outdoor temperatures taken for the Iraq climate depend on the locations with minimum and maximum temperatures recorded in 2019 (Table 3 and Fig. 1). Software EES is used to solve the equations of thermal and exergy analysis of all system components.

2. Model description

The AVCRS has four mechanical components. These components include the compressor, condenser, evaporator and expansion device (Fig. 2a with Table 4 showing the ACSU specification). The refrigerants are fluids that absorb heat during evaporation. These refrigerants

provide a cooling effect during the phase change from liquid to vapour. The refrigerant selection depends on the operating pressure and temperature. Fig. 2b shows a pressure–enthalpy (P–h) diagram for an AVCRS. In the P–h diagram, process (1–2) is the isentropic compression in the compressor. Processes (2–2 s), (2 s-3) and (3–4) are desuperheating, condensation and subcooling in the condenser, respectively. Process (4–5) shows isenthalpic throttling in the expansion device. Finally, processes (5–6) and (6–1) are evaporation and superheating in the evaporator, respectively. The following are assumed for the thermal and exergy analyses:

1. The state operation is steady.
2. The kinetic and potential energies are neglected.
3. Heat losses to or from the environmental are negligible.
4. The compression process is irreversible.
5. The isentropic efficiency is changed with the compression ratio (CR).
6. The throttling processes are taken as constant enthalpy.
7. The vapour leaving the evaporator is superheating ($T_1 = T_e + 10$ °C) [48].
8. The liquid leaving the condenser is subcooling ($T_4 = T_c - 10$ °C) [48].
9. The evaporator and condenser temperature change with the indoor and outdoor temperatures ($T_e = T_{indoor} - 15$ °C and $T_c = T_{outdoor} + 15$ °C). The indoor and outdoor temperatures range from 17 °C to 27 °C and 30 °C to 55 °C, respectively [44 49].
10. The pressure drop in all compounds of the system is ignored.

Table 1
Thermodynamic properties of the refrigerants R22, R134a and R-161 [21-23].

Refrigerants	Chemical Name	Molecular weight kg/kmol	Critical temperature °C	Critical pressure kPa	Boiling temperature °C	ODP	GWP Per 100 year
R-22	Chlorodifluoromethane	86.47	96.15	4990.00	−40.81	0.055	1810
R-134a	Tetrafluoroethane	102	101.06	4059.3	−26.07	0	1430
R-161	Fluoroethane	48.06	102.2	5090	−37.6	0	4

Table 2
Summary of the analytical methods for AVCRS.

Analytical method	Ref.	Alternative refrigerant	Replaced refrigerant	Application	Results
Exergy analysis	[24] 2009	–	–	Combined power and refrigeration cycle	The exergy efficiency of the system equals to 27.10% by using a genetic algorithm method.
	[25] 2015	R1234yf and R1234ze	R134a	Two evaporators	Refrigerant HFO-1234yf is a good alternative to 134a because it is environmentally friendly. Great exergy efficiencies are obtained with R134a and R1234ze. High exergy destruction occurs in the compressor.
	[26] 2017	Butane	–	Vapour compression refrigeration system Autocascade refrigeration cycle	The three parameters, namely, inlet mass, condenser and inlet temperatures, reduce the exergy destruction within 126%, 88% and 3.6%, respectively.
	[27] 2013	R600a	R134a	Domestic refrigerator	The total exergy destruction in a domestic refrigerator (0.025 kW) is 45.05% when working with R600a.
	[28] 2019	Propane	–	Subcritical refrigeration cycle	The exergy distribution in the refrigeration cycle depends on the condenser parameters. Any change of the optimal superheat temperature has an effect on the relative exergy of each component of the system.
Thermal analysis	[29] 2017	Mixture of R1270 and R290 (75/25 by mass %	R22	Window air conditioner	The power (0.98 kW/TR) and capacity of the mixture are similar to those of R22. The variation in the percentage of COP of the R127 and R290 (75/25) is approximately 0.9% compared with that of R22.
	[30] 2017	R431A, R410A, R419A, R134a, R1270, R290 and mixtures R134a, R1270 and R290	R22	Air conditioning applications	The COP of the mixture R134a/R1270/R290 (50/5/45 by mass) is 2.10% higher than those of R22, R431A, R410A, R419A, R134a, R1270 and R290. The COP of the mixture R134a/R1270/R290 (50/5/45 by mass %) is better than that of R22.
	[31] 2017	R-290 and R-600a	R-134a	Domestic refrigerators	A good COP is achieved with the mixture of 60% R290 and 40% R600a.
	[32] 2017	R290	R22	Standard vapour compression cycle	The COP of refrigerant R290 is small and lower than that of R22.
	[33] 2018	R134a, R407c, R22 and R404a	–	Heat pumps and refrigerators	The compressor working under the HP mode is a positive entropy change, and that at the refrigerator mode is a negative entropy change. The optimal charge amount of the refrigerator is 15%–25% lower than that under the HP mode.
Exergy and thermal analysis	[34] 2008	R502, R404A and R507A	–	Actual vapour compression refrigeration cycle	The COP of the system is higher in the R507A working refrigerant than those of R502 and R404A. The exergy efficiency improves by 0.8%–0.3% by using R507A at the condenser temperatures ranging between 40 °C and 55 °C.
	[35] 2015	Mixture R290/R600a	–	Domestic refrigerator-freezers.	The COP, total exergy destruction and exergy efficiency are better at working with the mixture R290/R600a compared with the cycle using R600a only.
	[36] 2016	R1234ze	R134a	Air cooled vapour compression chilled with water	The system using R1234ze has a lower exergy destruction than that with refrigerant R-134a under the same operating conditions.
	[37] 2017	R1234yf	R134a	Domestic refrigeration system	The optimal COP at R1234yf for the mass charges of 91, 98 and 105 g Refrigerant R123yf is not a better alternative to R134a because of the high exergy destruction in the system.
	[38] 2018	Mixture R290/R600a	–	Domestic refrigerator–freezers	Comparison between two cycles with and without subcooling vapour compression refrigeration. The results show that the COP and exergy efficiency with subcooling can be increased to 5.27% and 11.4%, respectively.
	[39] 2018	R1234yf, R1234ze and R134a	R134a	Vapour compression system	The refrigerant mixture 40% R134a + 22% R1234yf + 38% R1234ze is a satisfactory COP with exergy efficiency and a good alternative for R134a.
	[40] 2018	R600, R600a, R601, R601a, R602, RC318, C5F12, R152a, R236ea, R236fa, R245ca, R245fa, RE245cb2 and R1234ze(E)	–	Integrated organic Rankine cycle with vapour compression refrigeration	The total exergy destroyed in the system equals to 84.1 kW occurring in the condenser. This value is approximately 34.7% of the total exergy destroyed in the system. R602 has a good performance in the integrated organic Rankine cycle with vapour compression refrigeration.
	[41] 2019	Mixture R170/R290		Freezer application	The modified vapour compression refrigeration cycle achieves COP and exergy efficiency equal to 12.7% and 20%, respectively.
	[42] 2016	–	R22	Split air conditioning system	The exergy destruction in the compressor and expansion device increases with an increase in atmospheric temperature from 20 °C to 46 °C. The power and exergy of the compressor are enhanced by 47.1% and 24.5%, respectively. The atmospheric temperature is increased.

3

Table 2 (continued)

Analytical method	Ref.	Alternative refrigerant	Replaced refrigerant	Application	Results
	2016 [43]	R1234yf	R134a	Air conditioning system	The exergy efficiency, exergy destruction and entropy generation are better when working with R1234yf compared with an air conditioning system using R-134a.
	2014 [44]	R290, R407C and R410A	R22	Split air conditioning system	The COP of the split air conditioning system is higher in the R290 working refrigerant than those of R407C and R410A under high ambient temperatures.
	2020 [45]	R1234yf, R1234ze and R1233zd	R410A and R134a	Air conditioning system	The result shows that R1234yf, R1234ze and R1233zd are good alternatives for R134a and R410A.

Table 3
Maximum and minimum environmental temperatures of the Iraq climatic conditions for the summer season of 2019 [46,47].

Climatic region	Basrah	Nasiriyah	Baghdad	Rutbah	Kirkuk	Mosul
max	48 °C	44 °C	42 °C	38 °C	40 °C	41 °C
min	32 °C	26 °C	25 °C	22 °C	25 °C	26 °C

Fig. 1. Selected Iraq climatic conditions.
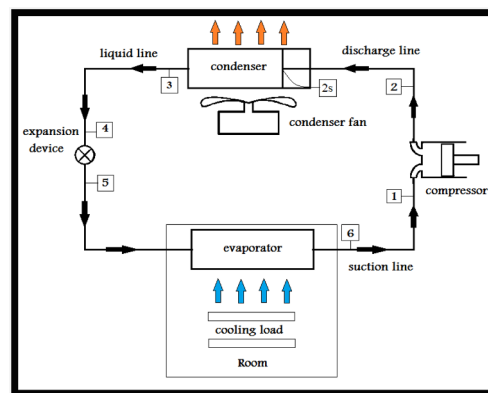
Fig. 2a. Split air conditioning unit.

Table 4
Specification of ACSU.

No.	Compounds	Specification
1	Compressor	Rotary
2	Condenser	Air cooled finned coil
3	Expansion device	Capillary tube
4	Evaporator	Air cooled finned coil
5	Capacity	7.032 kW

2.1. Thermal analysis

In this reversible process, the system and surroundings are returned to their first states at the end of the thermodynamic process. The reversible process can be achieved if the work and heat of the system are not exchanged with the surroundings. All real processes, such as
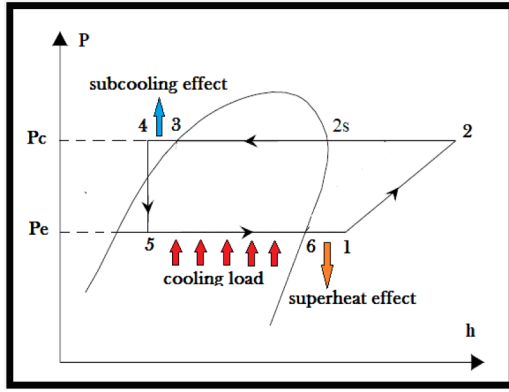
Fig. 2b. Pressure - enthalpy diagram.

AVCRS, are irreversible because heat is transferred across the compressor, condenser, evaporator and pipe of the cycle [50]. After the assumptions of the first law of thermodynamics are applied (Eq. [1]) in the ACSU analysis, the expression is as follows:

$$\frac{dE}{dt} = \sum_{in} \dot{m}\left(h + \frac{kE^2}{2} + gz\right) - \sum_{out} \dot{m}\left(h + \frac{kE^2}{2} + gz\right) + \dot{Q} + \dot{W}. \tag{1}$$

Compressor

The power of compressor equals: $\dot{W} = \dot{m}(h_2 - h_1)$ (2)

The CR of compressor is equal to $CR = \frac{P_{cond}}{P_{evap}}$, (2a)

The isontropic compreesor efficiency $\eta_c = \frac{h_{2s} - h_1}{h_2 - h_1}$, (2b)

The empirical efficiency is calculated as [51] : $\eta_c = 1 - 0.05CR$, (2c)

where the enthalpy can be found as h_1 = function (P_e and T_1) and h_{2s} = function (P_c and h_g).

Condenser

The rate of heat rejected in the condenser $\dot{Q_C} = \dot{m}(h_2 - h_4)$, (3)

where h_3 = function (P_c and h_f).

Expansion device

The throttling process is constant enthalpy$h_4 = h_5$, (4)

where $h_5 = h_4$, and h_4 = function (P_c and T_4).

Evaporator

$Q_{evap} = (h_6 - h_5)$, $\dot{Q}_{evap} = \dot{m}(h_6 - h_5)$, (5)

where the capacity of the ACSU is $\dot{Q}_{evap}$ = 7.032 kW [44], and h_6 = function (P_e and h_g).

COP

The COP is defined as the amount of cooling effect per unit work provided, and it can be expressed as follows:

$COP = \dot{Q}_{evap}/\dot{W}$. (6)

2.2. Exergy analysis

Exergy is the maximum available work that can be extracted from a system when it undergoes a process from its initial state to the state in equilibrium with its environment. Exergy is not a thermodynamic property. The exergy value depends on the states of the system and its environment. The power consumed by the AVCRS is always greater than that in the equivalent reversible one, and the difference is called exergy destruction or lost work. The exergy destruction is a part of the input power that is not converted into energy due to the irreversible

effect inside the ACSU. The exergy destruction can be obtained by computing the rate of entropy generation ($\dot{S}_{gen}$) [52]. The entropy generation and the work for a steady flow process are expressed according to the second law of thermodynamics [53]:

$$\dot{S}_{gen} = \frac{dS}{dt} - \sum_{i=0}^{n} \frac{\dot{Q}_i}{T_i} - \sum_{in} \dot{m}s - \sum_{out} \dot{m}s \geq 0, \tag{7}$$

$\dot{W}$

$$= \frac{d}{dt}(E - T_o S) + \sum_{i=0}^{n}\left(1 - \frac{T_o}{T_i}\right)\dot{Q} + \sum_{in} \dot{m}(h_{tot} - T_o.s) - \sum_{out} \dot{m}(h_{tot} - T_o.s) - T_o.\dot{S}_{gen}. \tag{8}$$

Exergy is a measure of the potential of an ACSU to convert the work as it undergoes a process from its original to a final state to ensure that it achieves equilibrium with its surroundings. After the ACSU and surroundings reach equilibrium, the ACSU will not change or be changed. This condition is known as the system dead state, and it has an exergy of zero. The dead state conditions for pressure P_o = 101.325 kPa, temperature $T_o = T_{outdoor}$ and friction dryer $x_o = 0$. The enthalpy and entropy are as follows: h_o and s_o = function (refrigerant, T_o and x_o).

The exergy expressions for the points in the ACSU are as follows:

$\Psi_o = h_o - (T_o s_o)$, (8a)

$\Psi_1 = h_1 - (T_o s_1) - \Psi_o$, (8b)

$\Psi_2 = h_2 - (T_o s_2) - \Psi_o$, (8c)

$\Psi_3 = h_3 - (T_o s_3) - \Psi_o$, (8d)

$\Psi_4 = h_4 - (T_o s_4) - \Psi_o$, (8e)

$\Psi_5 = h_5 - (T_o s_5) - \Psi_o$, (8f)

$\Psi_6 = h_6 - (T_o s_6) - \Psi_o$. (8g)

Compression processes 1 to 2: the rates of exergy destruction and efficiency of the compressor are as follows [54]:

$\Psi_{dest,comp} = (\Psi_1 - \Psi_2) + W = \dot{m}T_o(s_2 - s_1)$, (9)

$\eta_{dest,comp} = \frac{(\Psi_2 - \Psi_1)}{W} \times 100\%$. (9a)

Condensation processes 2 to 4: the rates of exergy destruction and efficiency of the condenser are as follows:

$\Psi_{dest,cond} = (\Psi_2 - \Psi_4) = T_o\dot{S}_{gen,cond}$ (10)

where the rate of entropy generation $\dot{S}_{gen} = \dot{m}\left[(s_2 - s_3) + \frac{\dot{Q}_{cond}}{T_{outdoor}}\right]$. (10b)

$$\eta_{dest,cond} = \frac{\dot{Q}_{cond}\left(1 - \frac{T_o}{T_{cond}}\right)}{\dot{m}[(h_2 - h_3 - T_o(s_2 - s_3)]} \times 100\%. \tag{10c}$$

Expansion processes 4 to 5: the rates of exergy destruction and efficiency of the throttling are as follows:

$\Psi_{dest,exp} = (\Psi_4 - \Psi_5) = \dot{m}T_o(s_5 - s_4)$, (11)

$\eta_{dest,exp} = -\frac{\Psi_4}{\Psi_5} \times 100\%$. (11a)

Evaporation processes 5 to 6: the rates of exergy destruction and efficiency of the evaporator are as follows:

$\Psi_{dest,evap} = (\Psi_5 - \Psi_6) = T_o\dot{S}_{gen,evap}$, (12)

$\dot{S}_{gen} = (s_6 - s_5) - \left[\frac{Q_{evap}}{T_{indoor}}\right]$, (12a)

$$\eta_{\mathbf{dest,evap}} = \frac{Q_{evap}\left(\frac{T_o - T_{indoor}}{T_{indoor}}\right)}{(h_5 - h_6 - T_o(s_5 - s_6))} \times 100\%. \qquad (12b)$$

The total exergy destruction is as follows:

$$\Psi_{\mathbf{dest,total}} = \Psi_{\mathbf{dest,comp}} + \Psi_{\mathbf{dest,cond}} + \Psi_{\mathbf{dest,exp}} + \Psi_{\mathbf{dest,evap}} \qquad (13)$$

$$\mathbf{or}\,\Psi_{\mathbf{dest,total}} = \mathbf{\dot{W}} - \Psi_{\mathbf{flow}} \qquad (13a)$$

The flow exergy: $\Psi_{\mathbf{flow}} = \dot{Q}_{evap}\left[\dfrac{T_o}{T_{indoor}} - 1\right].$ $\qquad (13b)$

The total efficiency: $\eta_{\mathbf{dest,total}}$

$$= \eta_{\mathbf{dest,comp}} + \eta_{\mathbf{dest,cond}} + \eta_{\mathbf{dest,exp}} + \eta_{\mathbf{dest,evap}}. \qquad (14)$$

A mathematical model was established for performing the thermal and exergy analysis of the ACSU by using EES programming software. Fig. 3 shows the flowchart for the EES solution procedure.
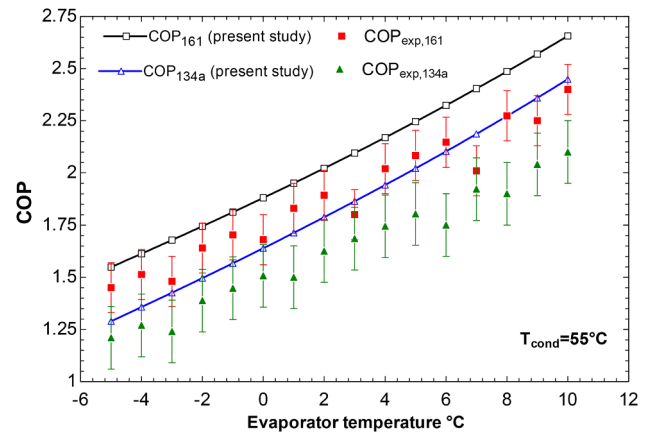
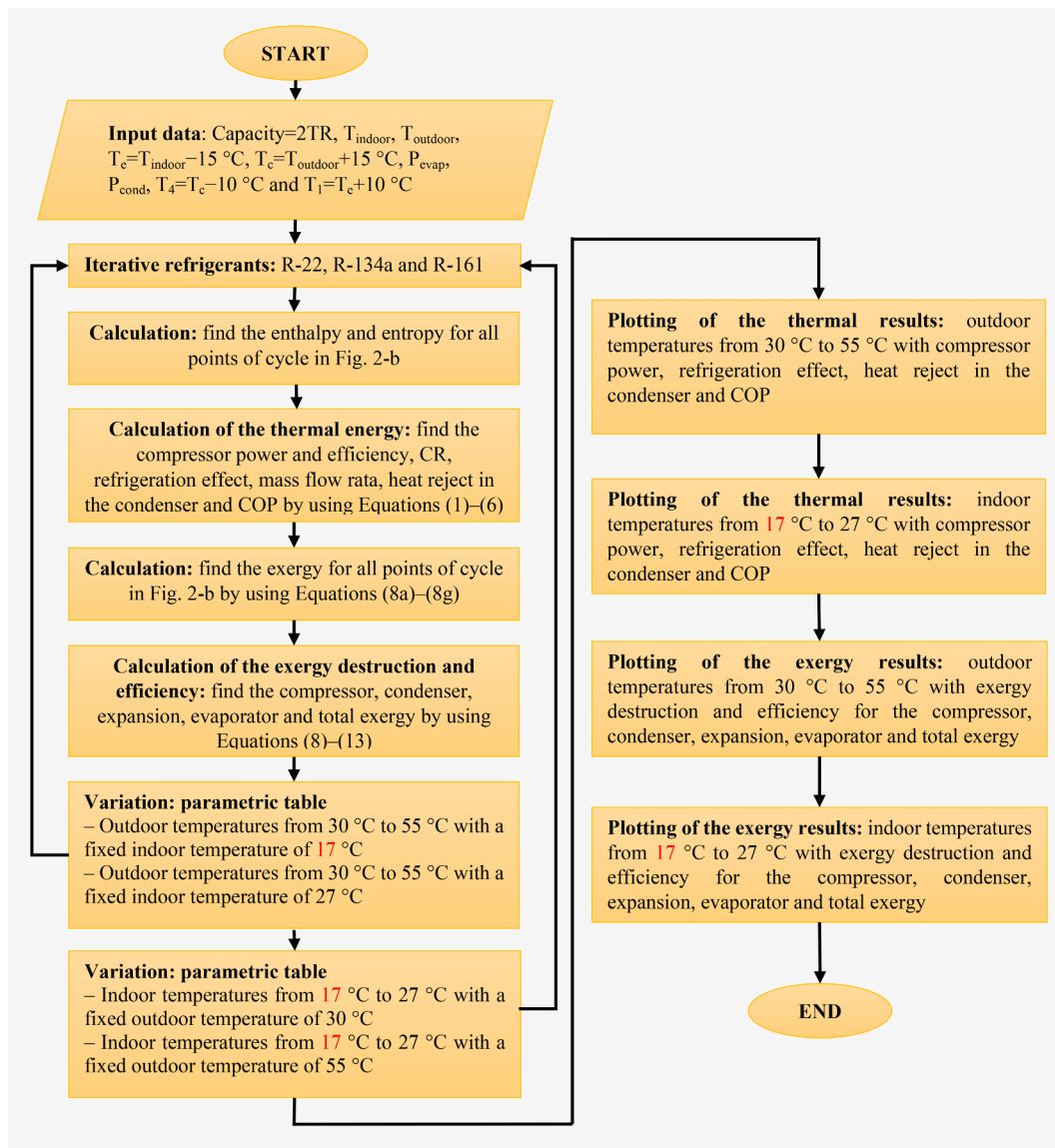**Fig. 4.** Validation of this study with the experimental data.

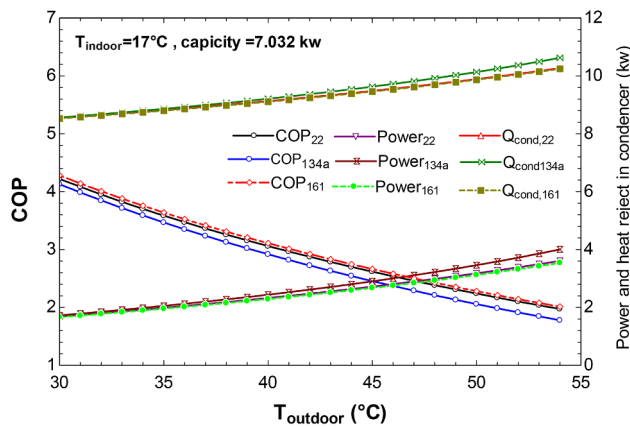**Fig. 3.** Flowchart of the EES solution procedure.

Fig. 5a. Effect of the outdoor temperature with COP, compressor power and heat rejection in the condenser; the indoor temperature is 17 °C.
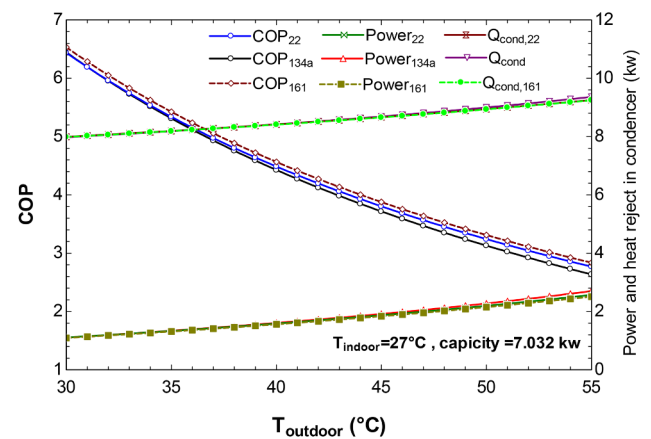

Fig. 5b. Effect of the outdoor temperature with COP, compressor power and heat rejection in the condenser; the indoor temperature is 27 °C.

3. Results and discussion

3.1. Validations

The effect of the condenser and evaporation temperature on the COP for R161 and R-134a is validated using the experimental data of AVCRS from Kalpesh et al. [55] to evaluate the accuracy of the results of this research (Fig. 4). The operating conditions' refrigeration capacity equals 2 TR, and the condenser temperature is 55 °C. The prediction of the COP in this study is slightly higher than that of the experiment results. The deviation between the compression results was because of the assumed constant thermal properties. Overall, the results for the present research have achieved good agreement with the experimental reading.

3.2. Effect of indoor and outdoor temperatures on the thermal performance

The COP, power of compressor and heat rejection in the condenser, as functions of the outdoor temperature, are illustrated in Fig. 5a. Any change in the outdoor temperature causes an increase in the condenser
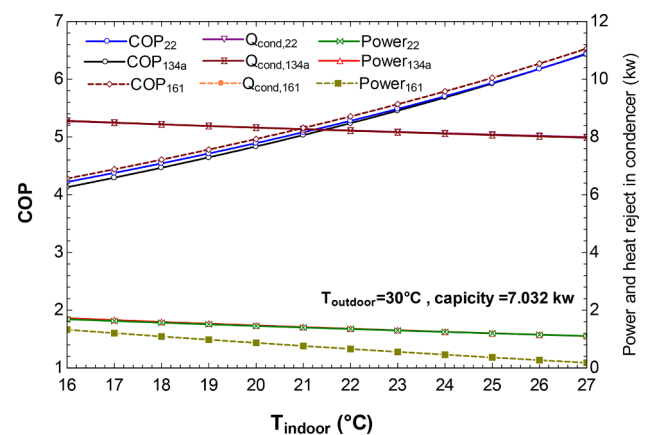

Fig. 6a. Effect of the indoor temperature with COP, compressor power and heat rejection in the condenser; the outdoor temperature is 30 °C.

Table 5
Thermal results of all compounds of the ACSU.

| Thermal results												
Compound of ACSU	Constant outdoor temperature = 45 °C Indoor temperatures						Constant indoor temperature = 17 °C Outdoor temperatures					
R-134a	17 °C	19 °C	21 °C	23 °C	25 °C	27 °C	30 °C	35 °C	40 °C	45 °C	50 °C	55 °C
Compressor [a]	2.789	2.582	2.394	2.221	2.063	1.916	1.658	1.976	2.348	2.789	3.324	3.984
Condenser [a]	9.521	9.322	9.142	8.977	8.827	8.688	8.498	8.787	9.123	9.521	10	10.59
Evaporator [b]	128.3	129.4	130.6	131.7	132.8	133.9	150.8	143.4	135.9	128.3	120.5	112.6
CR [−]	5.345	4.98	4.646	4.338	4.056	3.796	3.686	4.188	4.74	5.345	6.006	6.728
Mass flow [c]	0.0555	0.05502	0.05454	0.05407	0.05362	0.05317	0.04723	0.04966	0.0524	0.05552	0.0591	0.0632
COP [−]	2.553	2.758	2.975	3.206	3.452	3.716	4.295	3.604	3.034	2.553	2.143	1.788
R-22												
Compressor [a]	2.628	2.455	2.294	2.144	2.004	1.872	1.627	1.917	2.248	2.628	3.071	3.596
Condenser [a]	10.44	10.21	10	9.804	9.62	9.447	9.153	9.524	9.948	10.44	11.01	11.69
Evaporator [b]	142.6	143.3	144	144.7	145.4	146	162.6	156	149.4	142.6	135.6	128.5
CR [−]	4.57	4.288	4.028	3.788	3.565	3.358	3.255	3.657	4.095	4.57	5.084	5.641
Mass flow [c]	0.0499	0.0497	0.04946	0.04922	0.04899	0.04877	0.04381	0.04565	0.04768	0.04996	0.05252	0.0554
COP [−]	2.71	2.902	3.105	3.322	3.554	3.804	4.378	3.714	3.168	2.71	2.319	1.98
R-161												
Compressor [a]	2.583	2.411	2.252	2.104	1.966	1.837	1.604	1.889	2.212	2.583	3.014	3.523
Condenser [a]	9.371	9.205	9.053	8.911	8.779	8.656	8.471	8.734	9.031	9.371	9.763	10.22
Evaporator [b]	265.5	266.9	268.3	269.7	271	272.4	301.8	289.9	277.8	265.5	253	240.3
CR [−]	4.648	4.359	4.092	3.845	3.616	3.404	3.299	3.711	4.16	4.648	5.178	5.753
Mass flow [c]	0.0268	0.02668	0.02654	0.02641	0.02628	0.02615	0.0236	0.02457	0.02564	0.02682	0.02815	0.0296
COP [−]	2.757	2.954	3.162	3.384	3.622	3.877	4.441	3.771	3.22	2.757	2.363	2.022

Where [a] = kW, [b] = kJ/kg, [c] = kg/s.
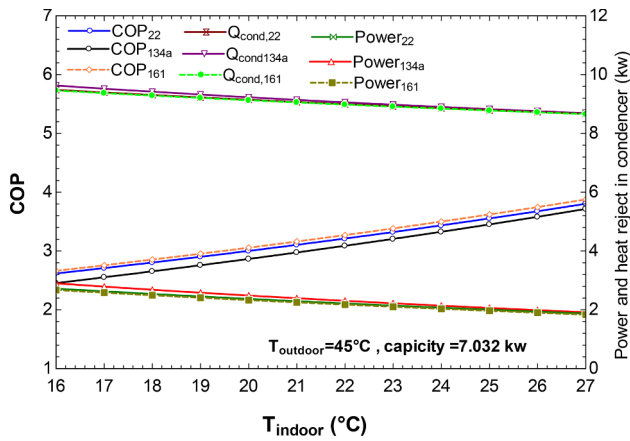
Fig. 6b. Effect of the indoor temperature with COP, compressor power and heat rejection in the condenser; the outdoor temperature is 45 °C.
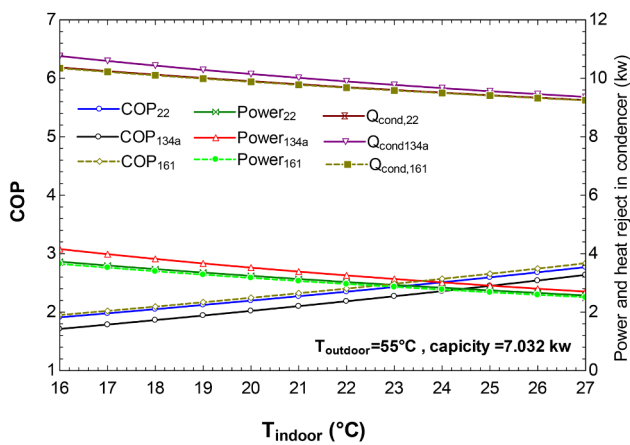

Fig. 6c. Effect of the indoor temperature with COP, compressor power and heat rejection in the condenser; the outdoor temperature is 55 °C.
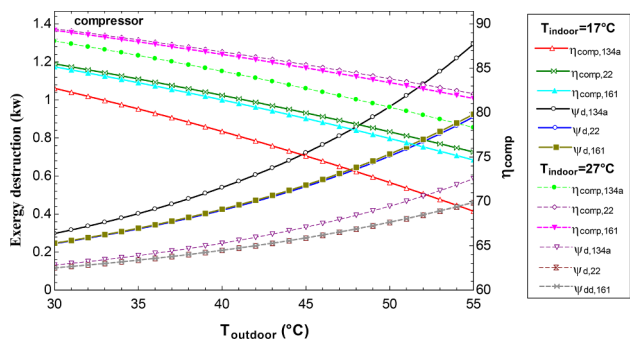

Fig. 7a. Outdoor temperature and compressor exergy destruction and efficiency; the indoor temperatures are 17 °C for refrigerants R-134a and R-22 and 27 °C for R-161.

Fig. 7b. Indoor temperature and compressor exergy destruction and efficiency; the outdoor temperatures are 30 °C for refrigerants R-134a and R-22 and 55 °C for R-161.

Fig. 8a. Outdoor temperature and condenser exergy destruction and efficiency; the indoor temperatures are 17 °C for refrigerants R-134a and R-22 and 27 °C for R-161.

temperatures due to $T_c = T_{outdoor} + 15$. The latent heat of condensation and COP decreased in all selective refrigerants at a constant indoor temperature of 17 °C. R-134a had a low COP, whereas R-161 had a slightly higher performance than R-22. This phenomenon is due to the higher refrigeration effect of R-161 than the other, and the compressor power is lower. The maximum outdoor temperature of the Iraqi climate (Table 3) ranges from 35 °C to 45 °C. The use of R-161 provides a more acceptable COP compared with those of R-22 or R-134a (Table 5). The compressor power and heat rejected in the condenser were positively affected with the increase in the outdoor temperatures at the indoor temperature of 17 °C. Fig. 5b shows that a slight effect on the
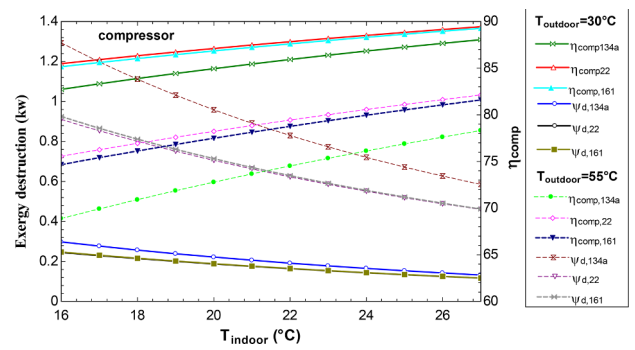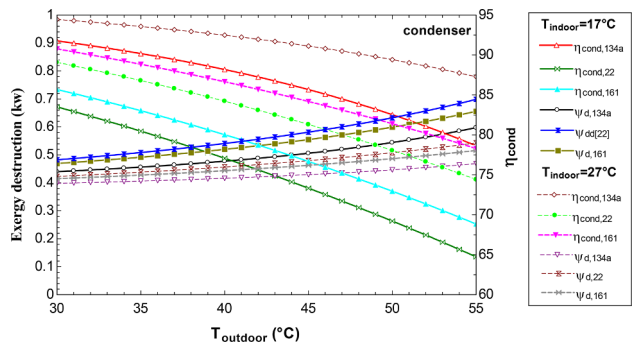
compressor power and heat rejection was observed at the indoor temperature of 27 °C due to the increase in the temperature of the evaporator from − 1 °C to 12 °C and the increase in the CR, thereby reducing the required mass flow rate of refrigerants. The objective of a condenser in an ACSU is to dissipate heat; therefore, a low COP is obtained when the dissipated heat (11 kW for 134a, 10.5 kW for R-22 and R-161) is high at the operating conditions of the outdoor and indoor temperatures of 55 °C and 17 °C, respectively. Figs. 6a and 6b show the variation of COP, power and heat rejected with the indoor temperature. The COP increased from 4.2 to 6.5 at a constant outdoor temperature and capacity of the ACSU with the increase in the indoor temperature from 16 °C to 27 °C. Moreover, the power and heat rejected were reduced. Refrigerant R134a had the highest compressor power (3.1 kW at an outdoor temperature of 55 °C) amongst all the selected refrigerants, and R-161 and R22 had equal values (Fig. 6c). The indoor temperature in the air conditioned area was maintained between 22 °C and 24 °C for a good refrigeration effect of the ACSU in the Iraq climatic conditions. This temperature within the comfort zone of the Iraqi environments is generally designated as the indoor design dry bulb temperature. The outdoor temperatures within the range between the lower limit of 38 °C and upper limit of 48 °C have been recorded in the summertime in a number of Iraqi cities (Table 3). The result shows a maximum refrigeration effect (3.877 kJ/kg) in the ACSU when the system was working with R-161.

3.3. Exergy efficiency and destruction

3.3.1. Compressor

The outdoor temperature affects the condenser temperatures, discharge temperatures and CR and the power consumed by the compressor. The stability point of the system changes with the increase in the outdoor temperature. This effect on the exergy destruction of the

Table 6
Exergy destruction for all compounds of ACSU.

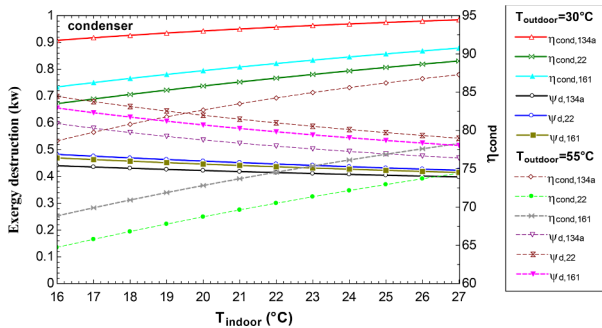| Exergy destruction (kW)												
Compound of ACSU	Constant outdoor temperature = 45 °C Indoor temperatures						Constant indoor temperature = 17 °C Outdoor temperatures					
R-134a	17 °C	19 °C	21 °C	23 °C	25 °C	27 °C	30 °C	35 °C	40 °C	45 °C	50 °C	55 °C
Compressor	0.6707	0.5802	0.503	0.4369	0.3801	0.331	0.2765	0.3739	0.5018	0.6707	0.8956	1.198
Condenser	0.4962	0.4787	0.4638	04.508	0.4394	0.4293	0.435	0.4467	0.469	0.496	0.531	0.5798
Expansion	0.4195	0.3836	0.3501	0.3187	0.2893	0.2619	0.1691	0.2343	0.3165	0.4195	0.5483	0.7096
Evaporator	0.4251	0.4192	0.4133	0.4076	0.402	0.3965	0.4051	0.4118	0.4184	0.4251	0.4318	0.4385
R-22												
Compressor	0.5112	0.4503	0.3971	0.3505	0.3095	0.2735	0.2291	0.3017	0.394	0.5112	0.6611	0.8537
Condenser	0.569	0.5468	0.5271	0.5095	0.4937	0.4794	0.4755	0.5002	0.5308	0.569	0.6173	0.679
Expansion	0.3662	0.338	0.3114	0.2863	0.2627	0.2404	0.1559	0.2117	0.281	0.3662	0.4707	0.599
Evaporator	0.4258	0.4198	0.4139	0.4082	0.4026	0.3971	0.4057	0.4124	0.4191	0.4258	0.4325	0.4392
R-161												
Compressor	0.5178	0.4553	0.4008	0.3533	0.3116	0.2749	0.2309	0.3047	0.3985	0.5178	0.6703	0.8663
Condenser	0.543	0.5234	0.5056	0.4897	0.4755	0.4627	0.4628	0.4842	0.5106	0.5436	0.5851	0.6378
Expansion	0.3433	0.3161	0.2904	0.2662	0.2435	0.222	0.1454	0.1982	0.2634	0.3433	0.4407	0.5591
Evaporator	0.4261	0.4202	0.4145	0.4089	0.4034	0.398	0.406	0.4127	0.4194	0.4261	0.4328	0.4395

Fig. 8b. Indoor temperature and condenser exergy destruction and efficiency; the outdoor temperatures are 30 °C for refrigerants R-134a and R-22 and 55 °C for R-161.
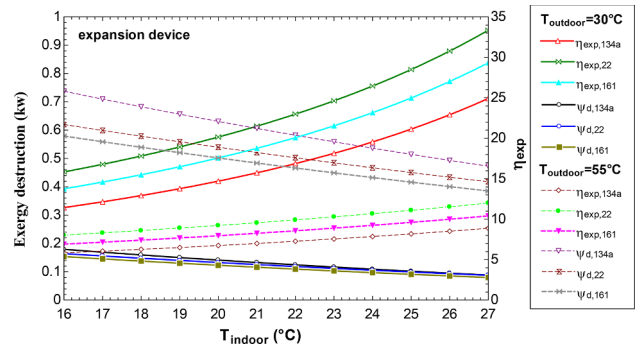

Fig. 9b. Indoor temperature and expansion device exergy destruction and efficiency; the outdoor temperatures are 30 °C for refrigerants R-134a and R-22 and 55 °C for R-161.
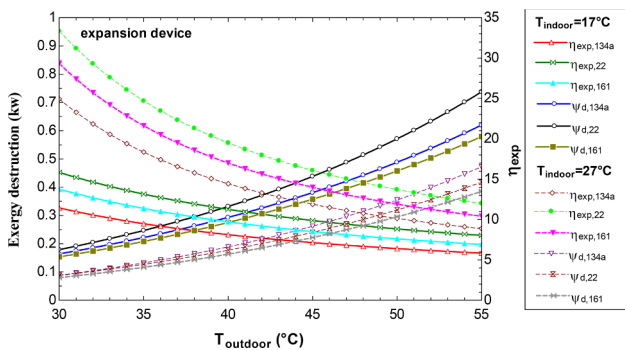

Fig. 9a. Outdoor temperature and expansion device exergy destruction and efficiency; the indoor temperatures are 17 °C for R-134a and R-22 and 27 °C for R-161.
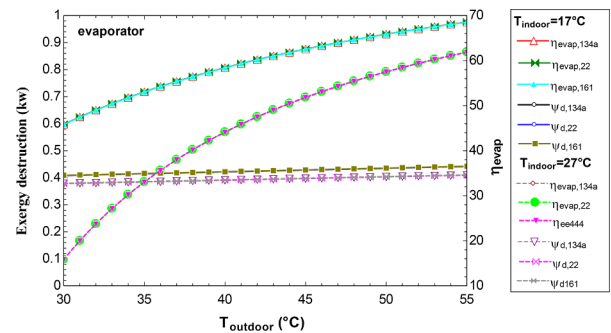

Fig. 10a. Outdoor temperature and evaporator exergy destruction and efficiency; the indoor temperatures are 17 °C for refrigerants R-134a and R-22 and 27 °C for R-161.

maximum exergy destruction occurred in the compressor amongst the components of the ACSU, which is similar to that in reference [8].

3.3.2. Condenser

Fig. 8a demonstrates that the entropy generation within the condenser increased with the increase in the outdoor temperature, thereby leading to increased destruction exergy and low condenser efficiency. This result is due to the low mass flow rate of the refrigerant and the increase in condensing temperature in all the refrigerants. Refrigerant R-161 had the lowest exergy destruction amongst the selective refrigerants, and R-134a had the highest value (Table 6). Fig. 8b shows
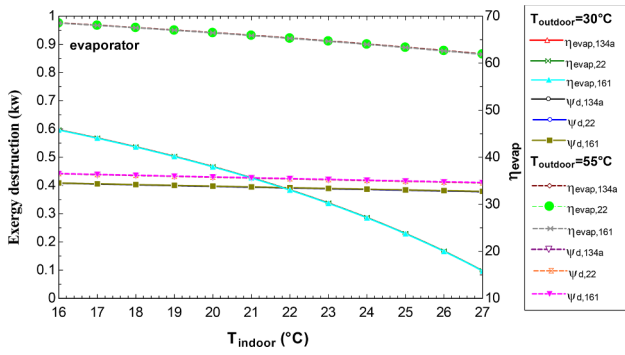
compressor is shown in Fig. 7a. A high exergy destruction (0.6707 kW) occurs in the compressor working with R-134a (Fig. 7b) under an indoor temperature of 16 °C to 27 °C because of the increase in suction and discharge temperature. The exergy efficiency of the compressor decreased to 70% for R-134a and approximately equalled 75% for R-161 and R-22 with the increase in the outdoor temperature from 30 °C to 55 °C. This result is due to the increase in the entropy generation and degree of superheating of the vapour refrigerant outlet compressor. The improvement in exergy efficiency of the compressor is approximately 22.3% because R-161 is replaced in the ACSU. The result shows that the

Fig. 10b. Indoor temperature and evaporator exergy destruction and efficiency; the outdoor temperatures are 30 °C for refrigerants R-134a and R-22 and 55 °C for R-161.
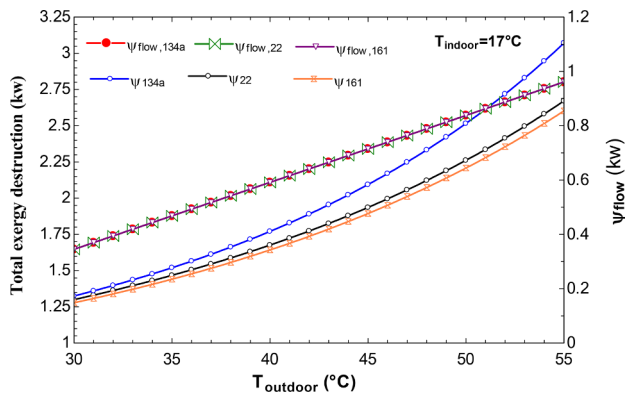

Fig. 11a. Variation of outdoor temperature and total exergy destruction in the ACSU and exergy flow; the indoor temperatures are 17 °C for refrigerants R-134a and R-22 and 27 °C for R-161.
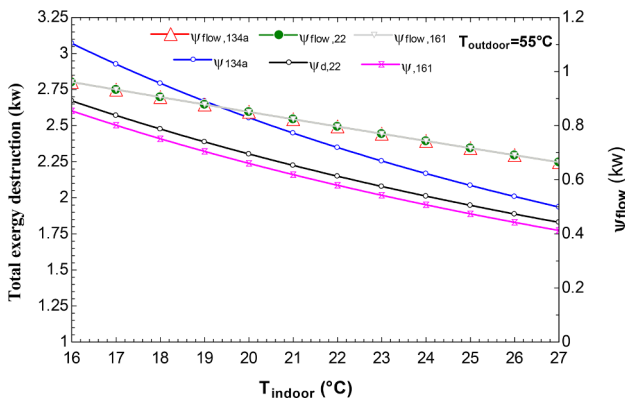

Fig. 11b. Indoor temperature and total exergy destruction in the ACSU and exergy flow; the outdoor temperatures are 17 °C for refrigerants R-134a and R-22 and 27 °C for R-161.

that the condenser exergy destruction in all refrigerants decreased with the increase in the indoor temperature. This phenomenon was because of the high temperature difference between the outdoor temperature and the refrigerant in the condenser. The optimum condensing temperature under the Iraq conditions is approximately 40 °C because this value can provide good exergy efficiency. In the low outdoor temperature, the exergy destruction in each refrigerant decreases. However, the exergy destruction increased in the low indoor temperature. The results show that the exergy destruction is high in refrigerants R-22 (0.6173 kW), R-161 (0.585 kW) and R-134a (0.531 kW) when the outdoor temperature increased to 50 °C. This result is attributed to the great difference between the outdoor temperature and the refrigerant.

The ACSU should be operated within the outdoor temperature of 30 °C–45 °C to obtain a good exergy destruction in the condenser.

3.3.3. Expansion device

The exergy destruction in the expansion device increased with the increase in the outdoor temperature increased (Fig. 9a). The ACSU working with R-134a had the highest exergy destruction, whereas R-161 showed the lowest value (Table 6). The exergy efficiency decreased with the increase in the outdoor temperature but increased when the indoor temperature increased (Fig. 9b). This increase resulted in an irreversibility and increase in the pressure difference between the inlet and the outlet of the expansion device. In this study, the CR varied from 3.6 to 6.7, 3.2 to 5.6 and 3.2 to 5.7 for R-134a, R-22 and R-161, respectively. The result shows the minimised exergy destruction occurred in the expansion device, out of all the ACSU components, due to the adiabatic expansion process. The R-161 showed a good performance according to the energy and exergy destruction of the ACSU. The exergy efficiency of R-161 increased from 8% to 11% with the increase in the indoor temperature. The indoor temperature varied from 16 °C to 27 °C (Fig. 9b).

3.3.4. Evaporator

Figs. 10a and 10b demonstrate that the outdoor temperature increases with a constant indoor temperature of 17 °C or 27 °C. The effect of exergy destruction is very small (between 0.38 kW and 0.42 kW) for all refrigerants. This phenomenon is due to the constant evaporator temperature along the evaporation process and the small effect of dryness fraction at the evaporator inlet. The change of indoor temperature has a 10% effect on the exergy efficiency. Exergy destruction increases with the decrease in the temperature of the evaporator. This phenomenon occurs because the heat transfer between the indoor space and the refrigerant decreases with the decrease in the evaporator temperature. Accordingly, the refrigerating effect and mass flow rate decrease; thus, the exergy destruction increases. In the low outdoor temperature, the exergy destruction for each refrigerant remains roughly the same. The results show that the entropy generation is lower in the evaporator than that in the condenser. This result is attributed to the refrigerant that undergoes an almost isothermal heat addition process during the phase change in the evaporator with a relatively small temperature difference between the evaporator and the indoor space.

3.4. Flow and total exergy

The variations of the outdoor temperature in the ACSU with flow exergy, which showed no change in all refrigerants, are shown in Fig. 11a. The change of the total exergy destruction is lowest for R-161 (2.1 kW), followed by R-22 and R-134a. The exergy flow in all working refrigerants does not change with the indoor and outdoor temperatures (Fig. 11b) because the capacity of the ACSU remains constant (2 TR). The exergy flow is positive with the indoor and outdoor temperature change. The results of the indoor and outdoor temperatures with total exergy destruction could be explained by the temperature difference between the inlet to the condenser temperature and the outlet from the evaporator. The high condenser temperature and pressure resulted in a great refrigerant mass flow rate and increased total exergy destruction.

4. Conclusions

The following effects were observed when refrigerants R-22 and R-134a of the ACSU were replaced with the new R-161:

– The increase in the outdoor temperature reduced the COP of the ACSU to 58.5% for R-134a, followed by 54.6% for R-22 and 54.5% for R-161. When the indoor temperature was reduced from 27 °C to 17 °C, the COP decreased to 31.4% (R-134a), followed by 29% (R-

22) and 28.1% (R-161).

- The increase in the outdoor temperature reduced the volumetric efficiency. Accordingly, the mass flow rate delivered by the compressor increased the compressor power to 3.98 kW (R-134a), followed by 3.59 and 3.52 kW for R-22 and R-161, respectively.
- The increased indoor temperature reduced the CR. Consequently, the mass flow rate outlet from the compressor decreased to 0.53 kg/s (R-134a), followed by 0.048 and 0.026 kg/s for R-22 and R-161, respectively.
- The exergy efficiencies of the condenser and compressor improved by 7.3% and 9.1%, respectively.
- The exergy efficiency of the ACSU was improved by 4.3%.
- The exergy destruction in the compressor was reduced by 7.4%.
- The exergy destruction in the condenser was increased by 9.2%.
- The varying indoor temperatures had a slight effect on the exergy flow for all tested refrigerants.
- Exergy destruction strongly depended on the indoor and outdoor temperatures.
- The ACSU with R-161 had the lowest exergy destruction and highest exergy efficiency compared with other refrigerants. Therefore, this refrigerant can be selected as an alternative to R-22 and R134a for Iraq climatic conditions.

CRediT authorship contribution statement

Ali Lateef Tarish: Conceptualization, Methodology, Writing - original draft. **Mushtaq Talib Hamzah:** Data curation, Visualization, Investigation. **Wasan Assad Jwad:** Software, Validation.

References

[1] B.O. Bolaji, Z. Huan, Ozone depletion and global warming: Case for the use of natural refrigerant–a review, Renew. Sustain. Energy Rev. 18 (2013) 49–54.
[2] Zhao Yang, et al., Research on the flammable characteristics of fluoroethane (R161) and its binary blends, Int. J. Refrig 56 (2015) 235–245.
[3] I. Dincer, M.A. Rosen, Exergy Analysis Of Heating, Refrigerating and Air Conditioning: Methods and Applications, Academic Press, 2015.
[4] Hüseyin Utku Helvacı, Gülden Gökçen Akkurt, Thermodynamic performance evaluation of a geothermal drying system, Progress in Exergy, Energy, and The Environment, Springer, Cham, 2014, pp. 331–341.
[5] M.M. Rashidi, N. Rahimzadeh, N. Laraqi, Evaluation of the equations of state for air, nitrogen and oxygen on throttle reduction efficiency by using exergy analysis, Int. J. Exergy 9 (3) (2011) 297–318.
[6] Y.A. Cangel, Michael A. Boles, Thermodynamics: An Engineering Approach 4th Edition in SI Units, McGraw-Hill, Singapore (SI), 2002.
[7] Mehmet Kanoğlu, Yunus A. Çengel, İbrahim Dinçer, Efficiency Evaluation of Energy Systems, Springer Science & Business Media, 2012.
[8] Jamal Uddin Ahamed, Rahman Saidur, Haji Hassan Masjuki, A review on exergy analysis of vapor compression refrigeration system, Renew. Sustain. Energy Rev. 15 (3) (2011) 1593–1600.
[9] Bayram Kılıç, Exergy analysis of vapor compression refrigeration cycle with two-stage and intercooler, Heat Mass Transf. 48 (7) (2012) 1207–1217.
[10] S. Devotta, A.S. Padalkar, N.K. Sane, Performance assessment of HCFC-22 window air conditioner retrofitted with R-407C, Appl. Therm. Eng. 25 (17-18) (2005) 2937–2949.
[11] W. Chen, A comparative study on the performance and environmental characteristics of R410A and R22 residential air conditioners, Appl. Therm. Eng. 28 (1) (2008) 1–7.
[12] Bukola Olalekan Bolaji, Performance investigation of ozone-friendly R404A and R507 refrigerants as alternatives to R22 in a window air-conditioner, Energy Build. 43 (11) (2011) 3139–3143.
[13] R. Llopis, et al., Experimental evaluation of HCFC-22 replacement by the drop-in fluids HFC-422A and HFC-417B for low temperature refrigeration applications, Appl. Therm. Eng. 31 (6-7) (2011) 1323–1331.
[14] Vedat Oruç, et al., Experimental comparison of the energy parameters of HFCs used as alternatives to HCFC-22 in split type air conditioners, Int. J. Refrig 63 (2016) 125–132.
[15] K. Harby, Hydrocarbons and their mixtures as alternatives to environmental unfriendly halogenated refrigerants: An updated overview, Renew. Sustain. Energy Rev. 73 (2017) 1247–1264.
[16] Madhu Sruthi Emani, Bijan Kumar Mandal, The use of natural refrigerants in refrigeration and air conditioning systems: a review, IOP Conference Series: Materials Science and Engineering 377 IOP Publishing, 2018.
[17] Yunchan Shin, et al., Performance characteristics of automobile air conditioning using the R134a/R1234yf mixture, Entropy 22 (1) (2020) 4.
[18] Rajendran Prabakaran, Dhasan Mohan Lal, Sukumar Devotta, Effect of thermostatic

[19] expansion valve tuning on the performance enhancement and environmental impact of a mobile air conditioning system, J. Thermal Anal. Calorim. (2020) 1–16.
[19] Atilla G. Devecioğlu, Vedat Oruç, Retrofitting of R-22 air-conditioning system with R1234ze (E), Environmentally-Benign Energy Solutions, Springer, Cham, 2020, pp. 87–96.
[20] Guy F. Hundy, Refrigeration, Air Conditioning and Heat Pumps, Butterworth-Heinemann, 2016, pp. 42–44.
[21] Reinhard Radermacher, Yunho Hwang, Vapor compression Heat Pumps With Refrigerant Mixtures, CRC Press, 2005.
[22] Handbook, A. S. H. R. A. E. "Fundamentals SI edition."American Society of Heating, Refrigerating and Air-Conditioning Engineers, Inc., Atlanta, GA 8 (1997).
[23] Xiaozhen Hu, Xianyang Meng, Wu. Jiangtao, Isothermal vapor liquid equilibrium measurements for difluoromethane (R32)+ trans-1, 3, 3, 3-tetrafluoropropene (R1234ze (E)), Fluid Phase Equilib. 431 (2017) 58–65.
[24] Yiping Dai, Jiangfeng Wang, Lin Gao, "Exergy analysis, parametric analysis and optimization for a novel combined power and ejector refrigeration cycle, Appl. Thermal Eng. 29 (10) (2009) 1983–1990.
[25] Alptug Yataganbaba, Ali Kilicarslan, İrfan Kurtbaş, Exergy analysis of R1234yf and R1234ze as R134a replacements in a two evaporator vapour compression refrigeration system, Int. J. Refrig. 60 (2015) 26–37.
[26] Sahar Asgari, A.R. Noorpoor, Fateme Ahmadi Boyaghchi, Parametric assessment and multi-objective optimization of an internal auto-cascade refrigeration cycle based on advanced exergy and exergoeconomic concepts, Energy 125 (2017) 576–590.
[27] Mahmood Mastani Joybari, et al., Exergy analysis and optimization of R600a as a replacement of R134a in a domestic refrigerator system, Int. J. Refrig. 36 (4) (2013) 1233–1242.
[28] Miquel Pitarch, et al., Exergy analysis on a heat pump working between a heat sink and a heat source of finite heat capacity rate, Int. J. Refrig. 99 (2019) 337–350.
[29] Sharmas Vali Shaik, T.P. AshokBabu., Thermodynamic performance analysis of eco friendly refrigerant mixtures to replace R22 Used in air conditioning applications, Energy Proc. 109 (2017) 56–63.
[30] Sharmas Vali Shaik, T.P. AshokBabu., Theoretical performance investigation of vapour compression refrigeration system using HFC and HC refrigerant mixtures as alternatives to replace R22, Energy Proc. 109 (2017) 235–242.
[31] Pilla, Tejaswi Saran, Experimental evaluation mechanical performance of the compressor with mixed refrigerants R-290 and R-600a, Energy Proc. 109 (2017) 113–121.
[32] C.S. Choudhari, S.N. Sapali, Performance investigation of natural refrigerant R290 as a substitute to R22 in refrigeration systems, Energy Proc. 109 (2017) 346–352.
[33] Afshari, Faraz, A thermodynamic comparison between heat pump and refrigeration device using several refrigerants, Energy Build. 168 (2018) 272–283.
[34] Akhilesh Arora, S.C. Kaushik, Theoretical analysis of a vapour compression refrigeration system with R502, R404A and R507A, Int. J. Refrig. 31 (6) (2008) 998–1005.
[35] Gang Yan, Chengfeng Cui, Yu. Jianlin, Energy and exergy analysis of zeotropic mixture R290/R600a vapor-compression refrigeration cycle with separation condensation, Int. J. Refrig. 53 (2015) 155–162.
[36] Jemaa, Radhouane Ben, Energy and exergy investigation of R1234ze as R134a replacement in vapor compression chillers, Int. J. Hydrogen Energy 42 (17) (2017) 12877–12887.
[37] Belman-Flores, et al., Energy and exergy analysis of R1234yf as drop-in replacement for R134a in a domestic refrigeration system, Energy 132 (2017) 116–125.
[38] Chen, Qi, et al., Theoretical study on a modified subcooling vapor-compression refrigeration cycle using hydrocarbon mixture R290/R600a. (2018).
[39] Kumar, Raj, Computational energy and exergy analysis of R134a, R1234yf, R1234ze and their mixtures in vapour compression system, Ain Shams Eng. J. 9 (4) (2018) 3229–3237.
[40] B. Saleh, Energy and exergy analysis of an integrated organic Rankine cycle-vapor compression refrigeration system, Appl. Therm. Eng. 141 (2018) 697–710.
[41] Gang Yan, Changxiang He, Yu. Jianlin, Theoretical investigation on the performance of a modified refrigeration cycle using binary zeotropic hydrocarbon mixture R170/R290, Int. J. Refrig. 94 (2018) 111–117.
[42] M. Bilgili, et al., Effect of atmospheric temperature on exergy efficiency and destruction of a typical residential split air conditioning system, Int. J. Exergy 20 (1) (2016) 66–84.
[43] Soudabeh Golzari, et al., Second law analysis of an automotive air conditioning system using HFO-1234yf, an environmentally friendly refrigerant, Int. J. Refrig 73 (2017) 134–143.
[44] Khalid A. Joudi, Qusay R. Al-Amir, Experimental assessment of residential split type air-conditioning systems using alternative refrigerants to R-22 at high ambient temperatures, Energy Convers. Manage. 86 (2014) 496–506.
[45] Khelifa Salhi, et al., Energetic and Exergetic performance of solar-assisted direct expansion air-conditioning system with low-GWP refrigerants in different climate locations, Arab. J. Sci. Eng. (2020) 1–14.
[46] Dr. Joel N. Myers. Entrepreneur's Encyclopedia of Entrepreneurs [online], AccuWeather. Available at: https://www.accuweather.com/en/iq/iraq-weather. [Accessed April 2020].
[47] Climatestotravel.com. Average weather, seasons, temperature, rainfall, sunshine hours, best time to go, what to pack, Pegasusweb Mirko Cecchini, Via Venezia 15, 43122 Parma - Italy. Companies Register of Parma, https://www.climatestotravel.com/climate/iraq.
[48] Ozbek, Arif, Exergy characteristics of a ceiling-type residential air conditioning system operating under different climatic conditions, J. Mech. Sci. Technol. 30 (11) (2016) 5247–5255.
[49] Jones, William Peter, Air Conditioning Engineering, Routledge, 2007, p. 82.

[50] Ibrahim Dincer, Refrigeration Systems and Applications, John Wiley & Sons, 2017.
[52] Recep Yumrutaş, Mehmet Kunduz, Mehmet Kanoğlu, Exergy analysis of vapor compression refrigeration systems, Exergy 2 (4) (2002) 266–272.
[53] Adrian Bejan, Advanced Engineering Thermodynamics, John Wiley & Sons, 2016.
[54] İbrahim Dinçer, Adnan Midilli, Haydar Kucuk (Eds.), Progress in Exergy, Energy, and The Environment, Springer, 2014.
[55] K.N. Kothale, S.D. Nimbalkar, Study of R-161 refrigerant as an alternate refrigerant to various other refrigerants, Int. J. Curr. Eng. Technol. 4 (4) (2016) 236–241.

Further reading

[51] Camelia Stanciu, et al., Exergy analysis and refrigerant effect on the operation and performance limits of a One stage vapor compression Refrigeration system, Termotehnica 1 (2011) 36–42.